



# Processing–structure–tribological property interrelationships of zinc titanate coatings grown by atomic layer deposition <sup>☆</sup>



V. Ageh, H. Mohseni, T.W. Scharf <sup>\*</sup>

Department of Materials Science and Engineering, University of North Texas, Denton, TX, USA

## ARTICLE INFO

Available online 1 November 2013

### Keywords:

Atomic layer deposition  
Oxides  
Friction  
Defects  
Dislocations  
Transmission electron microscopy (TEM)

## ABSTRACT

The growth defect structure and properties of the zinc titanate ( $Zn_xTi_yO_z$ ) coating system have been tailored via the selective variation of atomic layer deposition (ALD) parameters to obtain different crystallographic zinc titanate phases, namely hexagonal ilmenite  $ZnTiO_3$  and cubic spinel  $Zn_2TiO_4$ . Amongst the phases with textured or random grain orientations, the (104) textured  $ZnTiO_3$  coatings with a defective (low stacking fault energy) structure exhibited excellent tribological behavior for an oxide coating. Steady-state sliding friction coefficients of ~0.12 and ~0.2 were measured in humid air and dry nitrogen, respectively, even after ex situ annealing at 550 °C. High resolution TEM with selected area electron diffraction revealed that the (104) planes have extensive stacking faults bordered by partial dislocations, which serve as a pathway for dislocations to glide parallel to the sliding direction and hence achieve low interfacial shear/friction, i.e. “deck-of-cards” shear. These ternary coatings with low crystallographic shear strength exhibit ductile behavior during sliding contact and thereby generate smoother wear surfaces compared to brittle microcrystalline oxide coatings, and thus are a potential candidate for high temperature solid lubrication.

© 2013 Elsevier B.V. All rights reserved.

## 1. Introduction

The field of thin film materials science and engineering thrives basically on the intelligent tailoring of the structure of materials resulting in desired properties by subjecting them to various processing techniques for specified applications which could be electronic, structural, tribological, biomedical, etc. Processing of thin films can be divided into two general stages which include a) a pre-synthesis stage which involves all operations and procedures for controlling the parameters and conditions for the desired structure and properties before the synthesis or fabrication of a material, and b) post-synthesis stage which considers all necessary techniques for optimizing the desired structure and properties for intelligent materials design. Several tools and equipment have been designed and fabricated to successfully perform all operations required for both stages. Most of these tools are equipped with automated or manually controlled systems for the variation of several parameters both at the pre- and post-synthesis stages of coating processing. Different processing techniques are available for the different material types (metals, ceramics, semiconductors, composites, etc.) which may include material deposition optionally performed either by laser [1] or vapor deposition techniques (physical or chemical) [2], while others may include casting, forming, and sintering [3].

ALD is a unique type of chemical vapor deposition (CVD) technique that is used to deposit elements, binary compounds and more recently ternary compounds. As a chemical vapor phase coating deposition method, ALD is entirely based on alternate, self-limiting surface reactions [4]. A typical ALD process involves a sequence of alternate precursor pulsing into a reaction chamber followed by Ar or N<sub>2</sub> purging of the unreacted species or by-products. For every precursor pulsing/exposure step, the substrate surface is saturated with a monolayer of that precursor thus resulting in a self-limiting coating growth mechanism. Due to these unique features, alternate precursor pulsing, self-limiting reactions and separated reactions by purging, ALD results in high coating conformality and uniformity with an excellent control of coating thickness. The capability to coat sharp and buried interfaces, deposit multilayer and alloy structures and low temperature processing are further attributes of ALD [4–9].

The aim of this study is to demonstrate how ALD can tailor the microstructure of the zinc titanate ( $Zn_xTi_yO_z$ ) system through the variation of relevant parameters that determine the properties required for tribological applications. The zinc titanate system has three main crystallographic phases: ilmenite phase  $ZnTiO_3$ , a derivative structure of corundum which has both rhombohedral and hexagonal lattices, the cubic spinel phase  $Zn_2TiO_4$ , and the low temperature form and defect cubic spinel phase  $Zn_2Ti_3O_8$  [10–13]. These compounds have been widely investigated in an array of applications cutting across several industries, ranging from electronics, semiconductors to manufacturing. For example, researchers in the area of catalysis have reported the use of the cubic spinel  $Zn_2TiO_4$  as sorbent for the removal of sulphur from coal gasification product gases, and also in hot gas desulphurization

<sup>☆</sup> This manuscript is based on work presented at the Society of Vacuum Coaters 56th Annual Technical Conference in Providence, Rhode Island, April 20–25, 2013.

<sup>\*</sup> Corresponding author. Tel: +1 9408916837.

E-mail address: [scharf@unt.edu](mailto:scharf@unt.edu) (T.W. Scharf).

units at temperature range of 400–700 °C [11].  $Zn_2TiO_4$  has been used also as a component in dielectric compositions for dielectric materials [14]. Ilmenite  $h\text{-ZnTiO}_3$  has been considered a promising candidate for microwave resonator materials [15,16]. It is also a useful candidate for gas sensors [16] (for ethanol, NO, CO, etc.) catalysts [17] and paint pigments [18] and just recently the capacity of  $h\text{-ZnTiO}_3$  to function as a lubricious oxide for tribological applications has been investigated [19,20]. However, the tribological behavior of these coatings in both humid air and dry nitrogen is unknown as well as the solid lubrication mechanisms studied with advanced characterization techniques like focused-ion beam and high resolution transmission electron microscopies.

## 2. Experimental details

### 2.1. Atomic layer deposition

Si (100) substrates were cut and cleaned by ultra-sonication in acetone, methanol and de-ionized water for 15 min each. A Savannah 100 viscous flow hot wall single wafer ALD system (Cambridge Nanotech Inc.) was used with a reactor chamber/computer controlled interface. The reactor chamber has dimensions of 100 mm in diameter and 6 mm in height. The computer controlled interface is equipped such that the number of precursor fields can be increased or decreased depending on the desired material. Other parameters that can be varied on this interface include, pulse time, exposure time, purge time, deposition temperature, precursor temperature and number of cycles thereby providing a wide variety of processing options to tailor coating structures.

#### 2.1.1. Precursor selection

Important qualities such as appreciable volatility, ability to undergo aggressive and complete reactions with the oxidant, good growth rate and no self-decomposition are relevant considerations in the choice of ALD precursor. One such precursor, Tetrakis dimethylamido titanium IV (TDMAT), was used as the titanium source. Though its process temperature is between 90 and 250 °C, as compared to other precursors with larger process temperature range, its growth rate and appreciable volatility makes it more preferred for this work compared to  $TiCl_4$ . Diethyl Zinc (DEZ) was used as the zinc source and de-ionized  $H_2O$  as the oxidant for both metal precursors.

#### 2.1.2. Recipe generation

Different deposition parameters were varied for the zinc titanate system for the synthesis of both cubic spinel  $Zn_2TiO_4$  and the ilmenite  $ZnTiO_3$  phases. Table 1 lists the three deposition recipes for the 1:1, 2:1, and 3:1 ZnO:TiO<sub>2</sub> pulse sequence ratios. The DEZ was kept at room temperature and pulsed into the chamber at 0.015 s while unreacted/excess species were purged out with nitrogen at 5 s. No exposure time of the reactants was used since the substrates are flat, i.e. not high-aspect ratio materials, that would require long precursor exposure times to coat. After the metal pulse, DI  $H_2O$  was used as the oxidant at a 0.025 s pulse and 5 s purge. A precursor temperature of 75 °C, 0.1 s pulse and 5 s purge was used for TDMAT. The chamber deposition temperature was 200 °C for all recipes.

Typical growth/cycle (GPC) values are 2.2 and 1.7 Å/cycle for the 1:1 and 2:1 ZnO:TiO<sub>2</sub> pulse sequence ratios, respectively. The larger GPC for the 1:1 ZnO:TiO<sub>2</sub> pulse was due to the smaller purge time of 5 s resulting in more CVD-like growth, while the smaller GPC for the 2:1 ZnO:TiO<sub>2</sub> pulse was due to the larger purge time of 25 s resulting in more ALD-like growth. A previous study [19] also confirmed that a 5 s purge time resulted in larger GPC, since this was insufficient time to purge away all unreacted and excess precursor species before the next pulse/purge cycle, thus resulting in intermixing and CVD-like growth. Also listed in Table 1 are the ALD conditions for a 3:1 deposition ratio of TiO<sub>2</sub>:ZnO, similar to the work of Borgese et al. [13], which was selected to see if the higher TiO<sub>2</sub> had any effect on coating structure.

**Tab. 1**  
ALD growth recipes with varying ZnO:TiO<sub>2</sub> pulse sequence ratios.

| Precursor                      | Pulse (s) | Purge (s) | Cycles |
|--------------------------------|-----------|-----------|--------|
| <i>1 ZnO:1 TiO<sub>2</sub></i> |           |           |        |
| DEZ                            | 0.015     | 5         | 5128   |
| DI H O                         | 0.025     | 5         |        |
| TDMAT                          | 0.1       | 5         |        |
| DI H O                         | 0.025     | 5         |        |
| <i>2 ZnO:1 TiO<sub>2</sub></i> |           |           |        |
| DEZ                            | 0.015     | 25        | 1000   |
| DI H O                         | 0.025     | 25        |        |
| DEZ                            | 0.015     | 25        |        |
| DI H O                         | 0.025     | 25        |        |
| TDMAT                          | 0.1       | 25        |        |
| DI H O                         | 0.025     | 25        |        |
| <i>3 ZnO:1 TiO<sub>2</sub></i> |           |           |        |
| DEZ                            | 0.015     | 5         | 4679   |
| DI H O                         | 0.025     | 5         |        |
| DEZ                            | 0.015     | 5         |        |
| DI H O                         | 0.025     | 5         |        |
| DEZ                            | 0.015     | 5         |        |
| DI H O                         | 0.025     | 5         |        |
| TDMAT                          | 0.1       | 5         |        |
| DI H O                         | 0.025     | 5         |        |
| <i>3 TiO<sub>2</sub>:1 ZnO</i> |           |           |        |
| TDMAT                          | 0.1       | 15        | 1000   |
| DI H O                         | 0.015     | 15        |        |
| TDMAT                          | 0.1       | 15        |        |
| DI H O                         | 0.015     | 15        |        |
| TDMAT                          | 0.1       | 15        |        |
| DI H O                         | 0.015     | 15        |        |
| DEZ                            | 0.1       | 15        |        |
| DI H O                         | 0.015     | 15        |        |

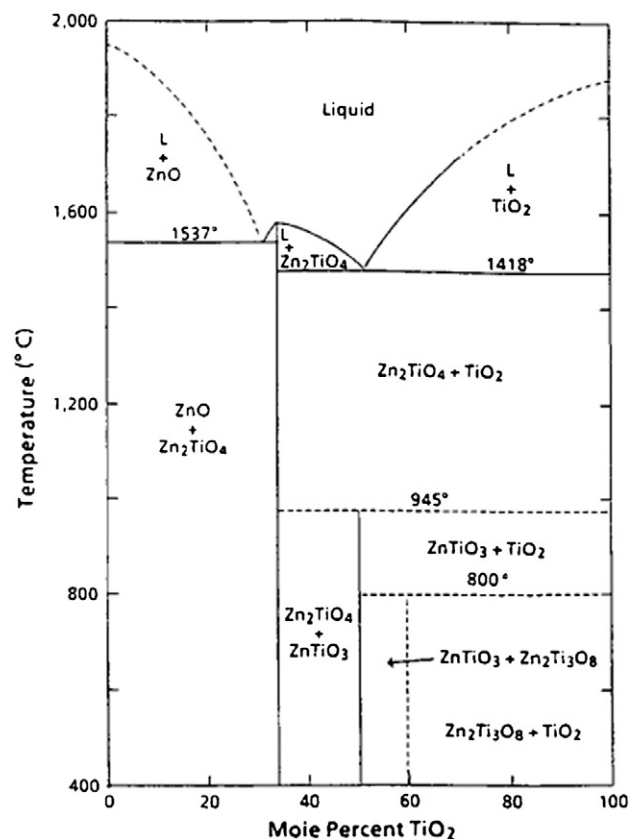


Fig. 1. ZnO-TiO<sub>2</sub> phase diagram [11]. Reprinted with permission.

Download English Version:

<https://daneshyari.com/en/article/8028117>

Download Persian Version:

<https://daneshyari.com/article/8028117>

[Daneshyari.com](https://daneshyari.com)